Int. J. Heat Mass Transfer. Vol. 32, No. 12, pp. 2385–2401, 1989
Printed in Great Britain

0017–9310/89 $3.00 + 0.00

Benefits of microgravity for measuring thermotransport coefficients in liquid metallic alloys

JEAN-PIERRE PRAIZEY
CEA/IRDI/DMECN/DMG/SEM, Laboratoire d'Etude de la Solidification, 85X,
F-38041 Grenoble Cedex, France

(*Received* 8 *June* 1988 *and in final form* 16 *February* 1989)

Abstract—After giving a brief review of thermotransport principles, this paper describes the experimental technique used and presents the results obtained on the ground. The author determines the solutal stability conditions to be satisfied by the metal alloy so that ground thermotransport measurements are not disturbed by convection effects. The benefits of microgravity when such conditions cannot be achieved are demonstrated and the results obtained on pure Sn (isotope separation), Sn–Co, Sn–Ag and Sn–Bi during Spacelab missions in 1983 and 1985 are presented. The results of experiments carried out without the disturbing effect of convection are compared with those found in the literature (experiments or calculations carried out from liquid structure models).

1. INTRODUCTION: OVERVIEW OF THE MAIN THERMOTRANSPORT DEFINITIONS

THERMOTRANSPORT, or the Soret effect, is the process whereby mass transport is induced by a temperature gradient. This process leads to separation of the liquid-phase alloy components. In a one-dimensional geometry, Fick's modified law is written as

$$J_i = D_i\left[\frac{\partial X_i}{\partial z} + S_i X_i \frac{\partial T}{\partial z}\right] \tag{1}$$

where T is the absolute temperature, z the sample axis, J_i the mass flow of component i, X_i the concentration of component i, S_i the Soret coefficient relating to component i, and D_i the diffusion coefficient of component i.

In that which follows, the same, non-indexed variables relate to the solute which is unique (log: Naperian logarithm).

When a steady state is reached, the following values can be defined ($\bar{X}$ being the mean concentration):

the thermotransport factor

$$r = \frac{\mathrm{d}\log(X/\bar{X})}{\mathrm{d}\log T}; \tag{2}$$

the Soret coefficient

$$S = \frac{\mathrm{d}\log(X/\bar{X})}{\mathrm{d}T} = r/T; \tag{3}$$

the heat of transport

$$Q = \frac{\mathrm{d}\log(X/\bar{X})}{\mathrm{d}\left(\frac{1}{RT}\right)} = -SRT^2 = -RrT$$

$$(R = 8.314\ \mathrm{J\ mol^{-1}\ K^{-1}}). \tag{4}$$

The experiments performed consisted in measuring $X/\bar{X}$ as a function of T, and calculating the r factor, independent of T as a first approximation.

2. DESCRIPTION OF EXPERIMENTAL SET-UP

The experiments are based on the 'shear cell' principle developed by Potard for isothermotransport measurements [1]. Its adaptation to thermotransport experiments is described in refs. [5, 6] (see Fig. 1).

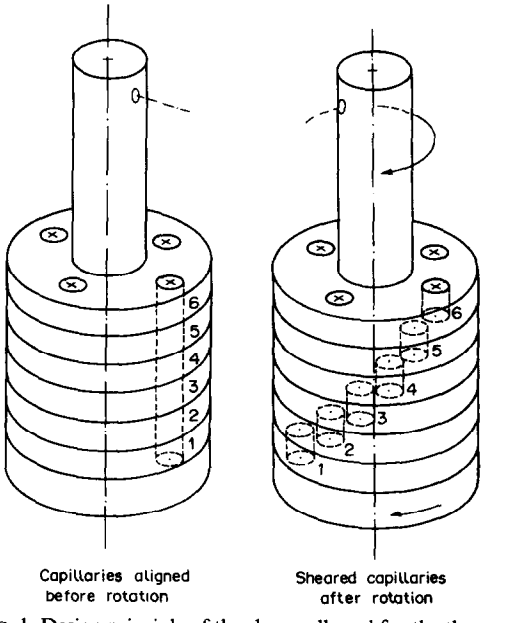

FIG. 1. Design principle of the shear cell used for the thermotransport experiments.

NOMENCLATURE

C thermotransport constant
D coefficient of mass diffusion, $(5\times10^{-5}\ \mathrm{cm^2\ s^{-1}})$
E_F Fermi energy [J]
k Boltzmann's constant [J K^{-1}]
h distance between two infinite parallel horizontal planes in Linden's model (cf. Section 4.1.1 (b)) [cm]
H distance between two infinite parallel vertical planes in Hart's model (cf. Section 4.2) [cm]
g acceleration due to gravity, 981 cm s^{-1}
Gr_S Grashof's solutal number, $(\gamma\beta_v(2R_s)^4/\nu^2)(\partial T/\partial z)$ with $\gamma\perp z$ at μg
Gr_T Grashof's thermal number, $(g\alpha_T R_s^3/\nu^2)\Delta T_R$ in vertical configuration at 1 g, $(\gamma\alpha_T(2R_s)^4/\nu^2)(\partial T/\partial z)$ with $\gamma\perp z$ at μg
J mass flow [g cm^{-2} s^{-1}]
K thermal diffusivity, 0.18 cm^2 s^{-1}
L sample length, 1.8 cm
m_1, m_2 atomic weights of solute and solvent [g]
Q transport heat [J mol^{-1}]
Q_m mass or intrinsic contribution to transport heat [J mol^{-1}]
Q_e electron or extrinsic contribution to transport heat [J mol^{-1}]
r solute thermotransport factor
R gas constant
R_s sample radius
Ra_S solutal Rayleigh number, $(g\beta_v/\nu D)R_s^4(\partial X/\partial z)$
Ra_T thermal Rayleigh number, $(g\alpha_T/\nu K)R_s^4(\partial T/\partial z)$
s equivalent ion diameter [cm]
S Soret coefficient, r/T [K^{-1}]
$\underline{S}$ coefficient defined in ref. [17], $(\beta_v/\alpha_T)\bar{X}(1-\bar{X})S$
T absolute temperature [K]
$\bar{T}$ mean sample temperature [K]
ΔT longitudinal temperature difference [K]
ΔT_R radial temperature difference [K]
V_c convection rate [cm s^{-1}]
V_d diffusion rate [cm s^{-1}]
V_N velocity (dimensionless) normalized by $g\alpha_T\Delta T_R H^2/\nu$ in Hart's analysis
x_1, x_2 atomic fractions of solute and solvent
X weight concentration
$\bar{X}$ mean weight concentration
X_{bot} separation coefficient defined in ref. [17]
ΔX weight concentration difference
z sample axis (pointing upwards in vertical position) [cm]
Z mean number of conduction electrons per alloy atom.

Greek symbols
α coefficient expressing the mass effect in equation (20), $\log(X/\bar{X}) = \alpha\log T+\beta T+C$
α_T thermal expansion coefficient
β coefficient expressing the electron effect in equation (20)
β_v solutal coefficient, $(\rho-\rho_{Sn})/\rho_{Sn}$
γ residual acceleration [cm s^{-2}]
δ inclination with respect to vertical [deg]
ρ density [g cm^{-3}]
ν viscosity of liquid Sn, $\nu(773\ \mathrm{K}) = 1.7\times10^{-3}\ \mathrm{cm^2\ s^{-1}}$.

The main features are described below.

(1) Four samples of 1.5 or 2 mm diameter and 18 mm length are placed in four longitudinal holes made in a cell consisting of six 3 mm thick disks.

(2) During the experiment, the sample, in its liquid state, is subjected to separation by thermotransport.

(3) When a steady chemical state is obtained after a time $\tau \geqslant 3L^2/\pi^2 D \approx 5.5$ h [5] each sample is divided *in the liquid state* into six parts by means of the thermomechanical device [6] controlling rotation of the cell disks.

For this type of experiment, the literature indicates that the sample is generally quenched and then analysed in the solid state. In such a case, there is a risk that the separation due to thermotransport will be disturbed by segregation due to solidification mechanisms.

(4) Each of the six parts isolated by this rotation is then analysed separately by neutron activation.†

3. GROUND EXPERIMENTS CARRIED OUT

Ground experiments were carried out with a stabilizing longitudinal temperature gradient for thermal convection (cold zone at the bottom).

The system is solute stabilizing if thermotransport carries the heaviest element downwards (case of Sn–Bi and Sn–Au systems) and solute destabilizing on the contrary (cases of Sn–Ag and Sn–Co systems).

† The method used at CENG (sample holder rotating in the 'Mélusine' irradiating reactor) enables each sample to be irradiated with the same flux. The concentration measurements are accurate to within a few thousandths to a few hundredths depending on the elements analysed.

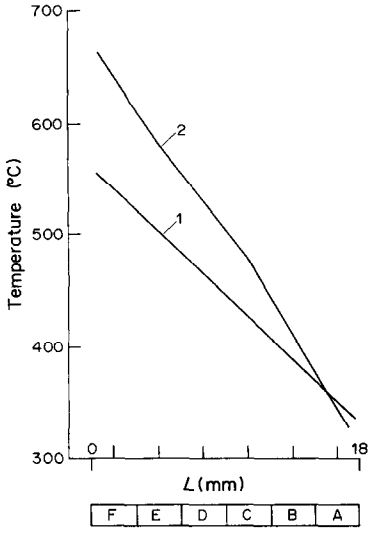

FIG. 2. Temperature profiles on the ground (1 g) and in microgravity (μg). (1) Experiments performed at 1 g in the cell charging furnace: all alloy systems apart from Sn–Co. (2) Experiments performed in the G.H.F. furnace: Sn–Co at 1 g; all systems in μg.

Two series of experiments were conducted on the ground:

(a) experiments on Sn–Co in zirconia cells containing 18 mm long, 2 mm diameter samples and treated in the 'GHF' furnace (see Section 6),

(b) experiments on other systems in graphite cells containing 18 mm long, 1.5 mm diameter samples and treated in the furnace used for filling the cells.

The temperature profiles of these two series of experiments are shown on Fig. 2 and are applied to the samples for a period of 24 h. The mean values of the thermotransport factor $r = [\mathrm{d}\log(X/\bar{X})]/[\mathrm{d}\log T]$ are given in Table 4 and on Figs. 6–11.

A simple linear regression has been made (without correction for change in scale) between $\log(X/\bar{X})$ and $\log T$ as $X/\bar{X}$ and T do not vary by a factor greater than 2.

The accuracy of the results for all analysed samples is given in ref. [9].

In the Sn–Au system, the effect of Au concentration on solutal stability was studied by taking measurements on two sets of samples: one set of two samples with Au content of 6×10^{-4} and another set of four samples with Au content of 6×10^{-2}.

Concentration measurements were taken by neutron activation for the first set of samples, and by atomic absorption for the second, the latter technique being feasible only when the concentration exceeds a certain percentage.

Figure 6 gives the results obtained:

$$\text{for } \bar{X}_1 = 6\times10^{-4},\quad r_1 = -0.182\pm0.036$$

$$\text{for } \bar{X}_2 = 6\times10^{-2},\quad r_2 = -0.574\pm0.050.$$

It will be shown in Section 4.3 that the value to be taken into account is the r_2 value.

A third set of two samples of Sn + 6% Au was tested in order to check that the duration $\tau = 5.5$ h (cf. Section 2) is sufficient to obtain a steady state.

A value of $r(5.5\text{ h}) = -0.574\pm0.022$ was obtained, to be compared with $r(24\text{ h}) = -0.574\pm0.050$.

4. CONVECTION ANALYSIS OF GROUND EXPERIMENTS

The simplest analysis consists in assuming zero radial temperature gradients and thus reducing the problem to consideration of just the vertical axis dimension. A solutal Rayleigh number value is then defined, depending on concentration, for which convection becomes negligible compared to diffusion (Section 4.1).

However, this approach is not sufficient as convection can be induced by the radial temperature gradients (Section 4.2.1).

The resultant convection can nonetheless be reduced by solute stabilization (Hart analysis [12], Section 4.2.2).

These three analysis stages are described in more detail below.

4.1. *One-dimensional calculation along vertical axis* [7] ($\Delta T_R = 0$)

4.1.1. *Stability threshold.*

(a) Solutal effect alone: the solutal Rayleigh number Ra_S is written as

$$Ra_S = \frac{g\beta_v}{vD} R_s^4\, \partial X/\partial z \tag{5}$$

or

$$\frac{\partial X}{\partial z} = S\bar{X}\frac{\partial T}{\partial z} = S\bar{X}\frac{\Delta T}{L} = \frac{r}{\bar{T}}\bar{X}\frac{\Delta T}{L} \tag{6}$$

Table 1. Calculation of $(Gr)_T$ for the different systems

System	R_s (mm)	ΔT_R (K)	$(Gr)_T = \{g\alpha_T R^3/\nu^2\}(\Delta T)_R$
Sn–Co	1.00	2/100	0.6
Other systems	0.75	1/100	0.12

such that

$$Ra_S = g\frac{(\Delta T)R_s^4}{\nu DL\bar{T}}\beta_v \bar{X}r. \quad (7)$$

A system is stabilizing for $\beta_v r < 0$ and therefore for $Ra_S < 0$. The stability condition is given by $Ra_S < Ra_{S1}$ with $Ra_{S1} = 67.4$ (Ostrounov solution [10]).

(b) Combined solutal and thermal effects: for a configuration confined by two infinite horizontal planes at a distance h apart, ref. [11] proposed the following stability condition:

$$Ra'_S = \frac{27\pi^4}{4} + Ra'_T \quad (8)$$

where

$$Ra'_S = \frac{g\beta_v}{\nu D}\frac{\partial X}{\partial z}h^4 \quad (9)$$

$$Ra'_T = \frac{g\alpha_T}{\nu K}\frac{\partial T}{\partial z}h^4. \quad (10)$$

The system is thermally stabilizing if $\partial T/\partial z > 0$, and thus if $Ra'_T > 0$. By analogy with relation (8), it is proposed to use the following expression for the cylindrical configuration:

$$Ra_S = 67.4 + Ra_T \quad (11)$$

in order to find the Ostrounov solution for $Ra_T = 0$

$$Ra_T = \frac{g\alpha_T}{\nu K}\frac{\partial T}{\partial z}R_s^4 = 272\frac{\partial T}{\partial z}R_s^4. \quad (12)$$

In the case of experiments on Sn–Co alloys, $Ra_T = 5$ whereas, in the other experiments, $Ra_T = 1$.

The value of the thermally stabilizing Rayleigh number therefore has virtually no effect on the position of the stability limit.

4.1.2. *Limit between convective and diffusive regimes.* The above examples concern the Ra_S limit value below which the fluid velocity is strictly zero. The Ra_S value for which the convection velocity V_c is equal to the diffusion velocity ($V_d = D/L$) will be greater than this limit value.

4.2. *Two-dimensional calculation*

4.2.1. *Influence of radial gradients.* It has been shown in ref. [7] that there is always a certain 'residual convection velocity' V_c due to radial temperature gradients and proportional to the radial Grashof number defined by

$$(Gr)_T = \frac{g\alpha_T R_s^3}{\nu^2}\Delta T_R. \quad (13)$$

References [13–15] propose the following expression for a cylindrical configuration:

$$\frac{V_c R_s}{\nu} = 3 \times 0.008(Gr)_T. \quad (14)$$

4.2.2. *Radial temperature gradient convection damping by solutal stabilization.* Hart [12] has dealt with this problem for a configuration confined by two parallel vertical planes separated by a distance H (see Fig. 3). This configuration could be extrapolated to the

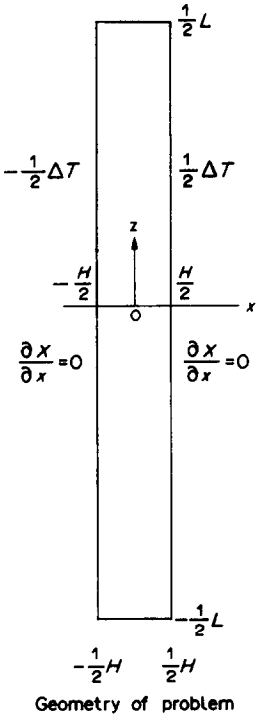

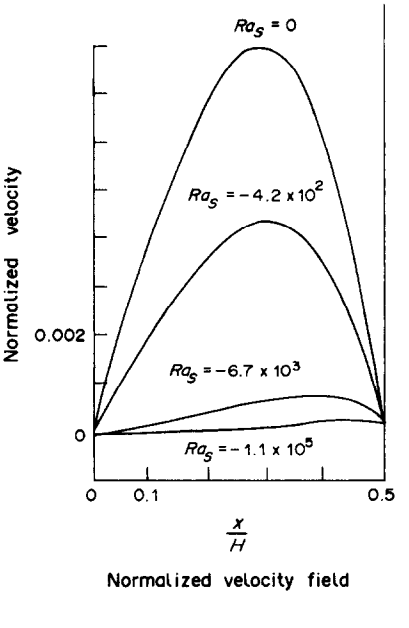

FIG. 3. Hart's hydrodynamic analysis [12]: thermal Rayleigh number, $Ra_T = g\alpha_T \Delta T_R H^3/K\nu$ = constant; solutal Rayleigh number, $Ra_S = (g\beta_v H^4 \partial X/\partial z)/D\nu$; V_N, velocity normalized by $g\alpha_T \Delta T_R H^2/\nu$.

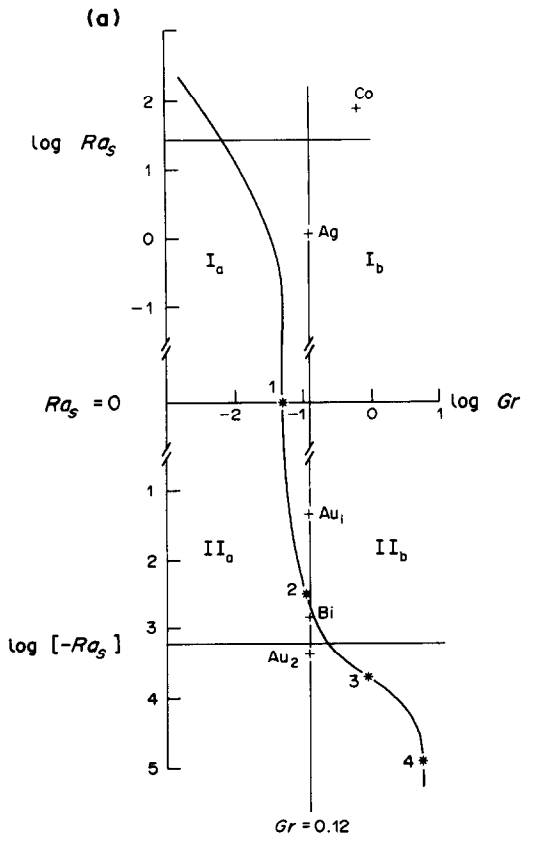

FIG. 4. (a) Limit of convective and diffusive regimes in an Ra_S, Gr diagram: $Ra_S = (g\Delta TR_s^4/VDL\tilde{T})\beta_v r\tilde{X}$; $Gr = (g\alpha_T R_s^3/v^2)\Delta T_R$; 1, 2, 3, 4, points calculated from Hart's analysis for which $V_c = V_d$. Zone I, solutal destabilizing systems: I_a diffusive regime; I_b convective regime. Zone II, solutal stabilizing systems: II_a diffusive regime; II_b convective regime.

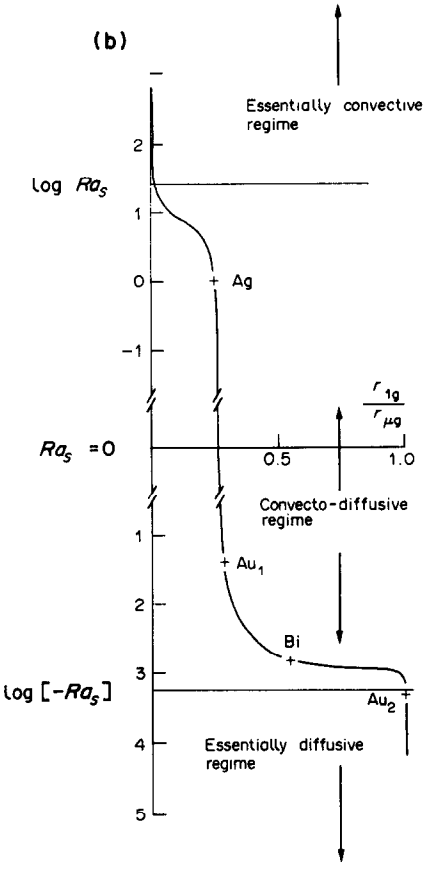

FIG. 4. (b) Separation efficiency on the ground as a function of solutal Rayleigh number for a constant Grashof number of $Gr = 0.12$.

cylindrical configuration by taking $H = R_s$ as the characteristic distance and by multiplying the velocity field by 3 in order to obtain relation (14) for $Ra_S = 0$.

The velocity V_N shown on Fig. 3 is standardized by $g\alpha_T\Delta T_R H^2/v$. Its maximum value will be considered for the calculation of V_c which can be expressed in terms of $(Gr)_T$ as

$$V_c = 3(Gr)_T(V_N)_{max}\frac{v}{H}. \tag{15}$$

The limit for which $V_c = V_d = D/L$ is such that

$$(Gr)_T = \frac{1}{3(V_N)_{max}}\frac{D}{v}\frac{H}{L}. \tag{16}$$

Thus, for the four values of Ra_S indicated by Hart, the corresponding $(Gr)_T$ values can be given. This leads to the graph shown on Fig. 4 indicating the limit separating the diffusive and convective domains.

4.3. *Situation of experimental points with respect to diffusive and convective domains*

4.3.1. *Order of magnitude of radial temperature gradients and corresponding Grashof numbers* $(Gr)_T$. Radial temperature gradients in the sample are due essentially to the different conductivities of the sample and crucible. To minimize these gradients, and thus limit convection effects, the following measures can be taken:

- choose a crucible with conductivity value close to that of the sample: however, in such cases, problems of chemical compatibility, machining and mechanical strength restrict the available choice and, in any case, the conductivities cannot be the same over the entire temperature range studied.
- reduce sample diameter, although, for technological reasons, it is difficult to have diameters smaller than 2 mm for zirconia crucibles and 1.5 mm for graphite crucibles, these being the dimensions used in the experiments described here.

Smaller diameters referred to in the literature are for quartz crucibles of 0.5 mm i.d. [29] (see Appendix C). In this case, surface diffusion (edge effects) may no longer be negligible [33].

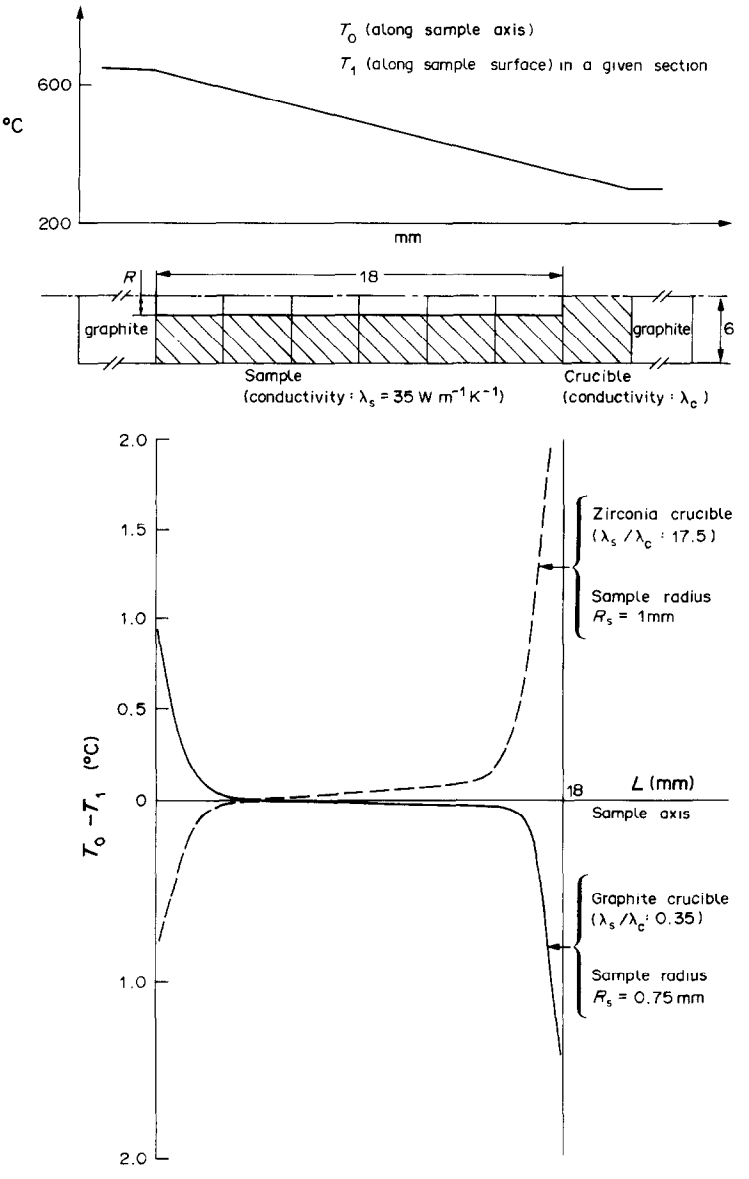

FIG. 5. Radial temperature deviation in the sample with respect to the ratio of sample/crucible thermal conductivities.

A two-dimensional calculation was made to determine the radial thermal deviations ΔT_R of the samples: ΔT_R varies from one end of the sample to the other (Fig. 5) with an order of magnitude of 10^{-2} K for the most part. For calculation of $(Gr)_T$, a value of 2×10^{-2} K will be taken for Sn–Co and 10^{-2} K for the other systems (Table 1).

4.3.2. *Order of magnitude of solutal Rayleigh numbers* Ra_S. The value of the thermotransport factor r must be known in order to calculate Ra_S

$$Ra_S = g\frac{(\Delta T)R_s^4}{vDL\bar{T}}\beta_v \bar{X} r. \qquad (17)$$

This value is also needed to determine the corresponding experimental point placed on Fig. 4(a), as shown in Section 7.

However, the following cases should be noted.

(a) Case of Sn–Co solutal destabilizing system

As Ra_S is positive, the representative point of the system in Fig. 4(a) must necessarily be located in the convective zone regardless of the value of the mean concentration $\bar{X}$.

(b) Case of Sn–Au solutal stabilizing system

Assuming at the outset that the value of r is that obtained for the concentration $X_2 = 6\%$ ($r = -0.574$), the following values can be calculated:

$$Ra_S(X_1) = -27$$

$$Ra_S(X_2) = -2700.$$

Table 2. Calculation of $(\Delta T_R)_{lim}$ giving a component separation efficiency better than 99%

System	Separation parameter $\underline{S} = -\{\beta_v/\alpha_T\}\bar{X}(1-\bar{X})r/\bar{T}$	$(\Delta T_R)_{lim} = 1.45\underline{S}$ (K)
^{112}Sn in pure Sn	7.25×10^{-4}	10^{-3}
Au ($\bar{X}_1 = 6\times10^{-4}$) in Sn	7.50×10^{-3}	10^{-3}
Bi ($\bar{X} = 4\times10^{-2}$) in Sn	2.09×10^{-1}	0.3
Au ($\bar{X}_2 = 6\times10^{-2}$) in Sn	7.50×10^{-1}	1

Referring to Fig. 4(a), it is found that, for the X_1 content, the r measurement is affected by convection whereas, for the X_2 content, it is not (thereby justifying consideration of the latter measurement of r for calculation of Ra_S values).

4.4. *Interpretation of ground experiments on stabilizing systems on the basis of Henry's three-dimensional calculation results* [16] (*see Appendix A*)

In ref. [16], Henry studied the effect of the radial gradient for a solutal stabilizing system. He showed that a component separation efficiency better than 99% is obtained for $\Delta T_R < \Delta T_{R\,lim}$. The $\Delta T_{R\,lim}$ values are given in Table 2.

The value of ΔT_R in the present experiments is of the order of 10^{-2} K. For the first two systems in the above table, $\Delta T_R > (\Delta T_R)_{lim}$ thereby explaining why these systems are highly disturbed by convection.

For the last two systems given in the table, $\Delta T_R < (\Delta T_R)_{lim}$ thereby explaining why these systems are not at all or only slightly disturbed by convection.

4.5. *Case of systems studied in the literature*

For most of these systems the mean contents are very low (a few p.p.m.), especially because the measuring technique generally uses a radioactive tracer. Moreover, the authors often wish to study a very diluted system in order to facilitate theoretical interpretation. As a result, $|Ra_S|$ is too small and, even for stabilizing systems, the alloy is in the convective zone in Fig. 4(a). This explains the dispersion and apparent incoherency of numerous results, a point that will be discussed in further detail in Section 8.

5. NEED TO CARRY OUT EXPERIMENTS IN MICROGRAVITY

It has already been mentioned that the following conditions must be satisfied in order for ground experiments to remain unaffected by convection:

- the system must be solutal stabilizing: in Section 8 it will be seen that this is the case for most of the systems,
- solutal stabilization must be sufficient, i.e. $Ra_S < -10^{-3}$, thus implying a *sufficient mean concentration* $\bar{X}$ (e.g. several percent for the Sn–Au system).

The possible ground experiment measurements are therefore limited to solutal stabilizing systems in which the concentration is only a few percent. However, the solute solubility may not allow such a concentration value to be obtained. Furthermore, if the concentration is greater than 1%, the 'diluted alloy' hypotheses generally used in theoretical interpretations are not totally justified.

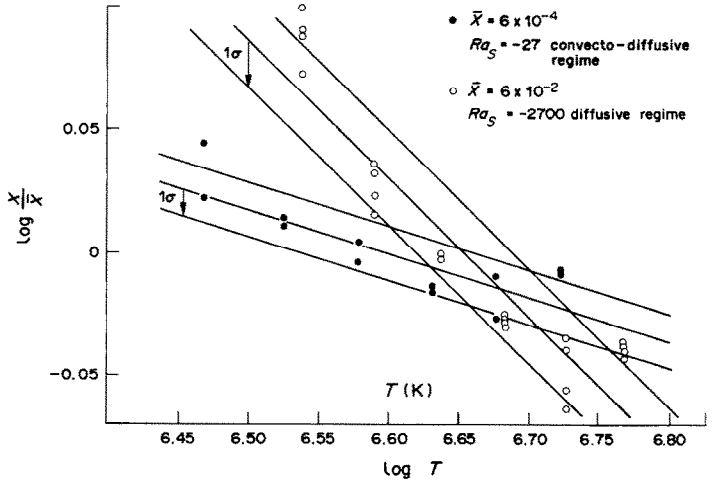

FIG. 6. Relative concentration of Au in Sn–Au as a function of temperature for two values of solutal Rayleigh number.

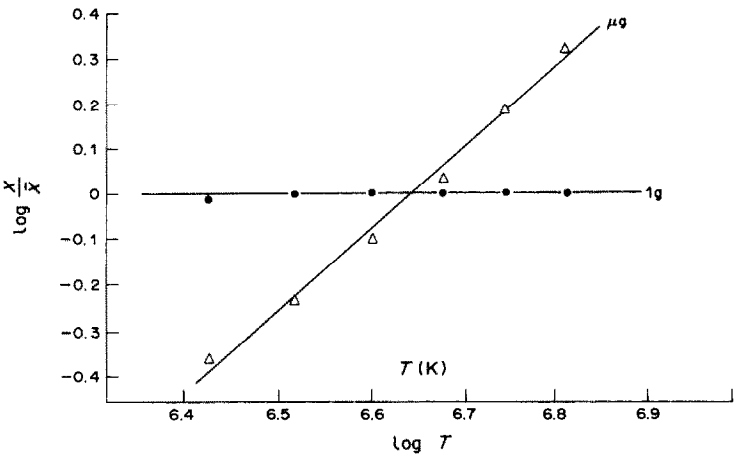

FIG. 7. Relative concentration of ^{59}Co in Sn–Co as a function of temperature at 1 g and in μg.

In the case of solutal destabilizing or insufficiently stabilizing systems (solute concentration too low), measurement of the thermotransport coefficients will be possible only under microgravity conditions.

6. EXPERIMENTS CARRIED OUT IN MICROGRAVITY

6.1. *Experimental conditions*

These experiments were performed in the G.H.F.† during *two Spacelab missions.*

● During the FSLP mission (First SpaceLab Payroll) in December 1983, measurements were taken on the Sn–Co system [7]. Thanks to the large number of samples (24 in a total of 3 cells), satisfactory measurement statistics were obtained with an accuracy of about 1% on the results.

● During the D1 mission (first German flight) in November 1983, measures were taken on the following:

—isotopic separation of tin by thermotransport;
—the Sn + εAg system for which ground results are available;
—the Sn + εBi system studied elsewhere in the *Mephisto* project.

● Given the number of systems studied, only a limited number of results are available for each system.

References [8, 9] give details of these experimental procedures.

In view of the limited electrical power available [6], zirconia cells were used, each with three 2 mm diameter, 18 mm long samples.

†The G.H.F. furnace (Gradient Heating Facility), built under CNES engineering responsibility, was also used for most of our laboratory experiments in the FSLP and D1 flights.

For all the experiments, the temperature profile is very similar to that shown on Fig. 2. The exact values measured for each cell are given in refs. [7–9].

6.2. *Overall results obtained in microgravity*

All the thermotransport coefficients measured during the FSLP and D1 missions are given in Table 4.

Table 4 together with Figs. 7–11 indicate the accuracy of the results. The confidence interval at ± 1 standard deviation σ is indicated on the figures.

Compared to the FSLP results on Sn–Co (r measured to within 2%), the D1 results are less accurate for three main reasons:

● the experimental difficulties, as discussed in ref. [9] and the number of systems studied were such that, for each system, only a limited quantity of results was available,

● activity measurement of ^{60}Co, originating from ^{59}Co, is easier than activity measurement of ^{113}In, originating from ^{112}Sn and ^{110m}Ag originating from ^{109}Ag; bismuth can be analysed only by chemical methods with an accuracy of the order of 10%,

● but above all, the relative variation of concentrations in the temperature range studied is only a few percent for ^{112}Sn and ^{109}Ag and 30% for Bi, whereas it is 70% for Co.

6.3. *Convection analysis in experiments performed in microgravity*

6.3.1. *Simplified order-of-magnitude analysis* [7]. The most adverse configuration is that where the residual acceleration γ is perpendicular to the z-axis of the sample.

For such a configuration, we have [13]

$$\frac{V_c \times 2R_s}{\nu} = 0.008(Gr)_T.$$

The Grashof limit for which $V_c = V_d = D/L$ is such

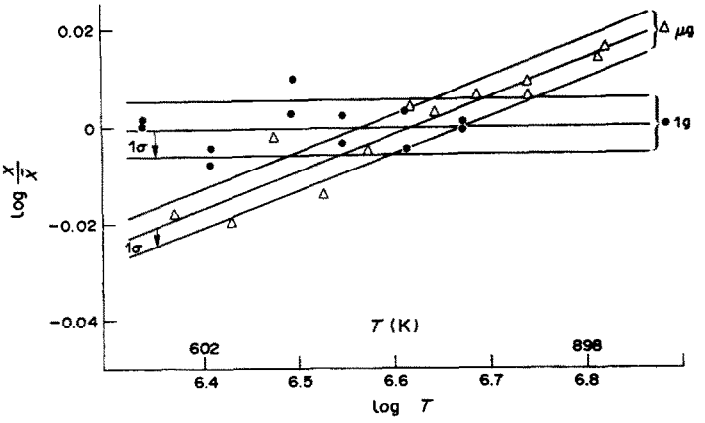

FIG. 8. Relative concentration of ^{112}Sn in pure Sn as a function of temperature at 1 g and in μg.

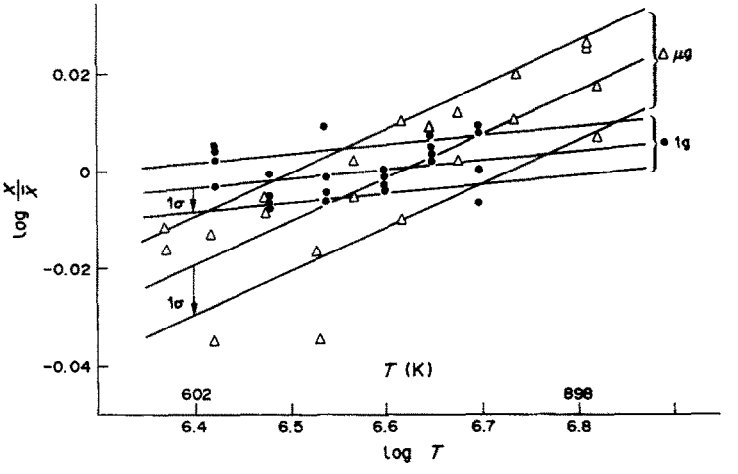

FIG. 9. Relative concentration of ^{112}Sn in Sn–Ag as a function of temperature at 1 g and in μg.

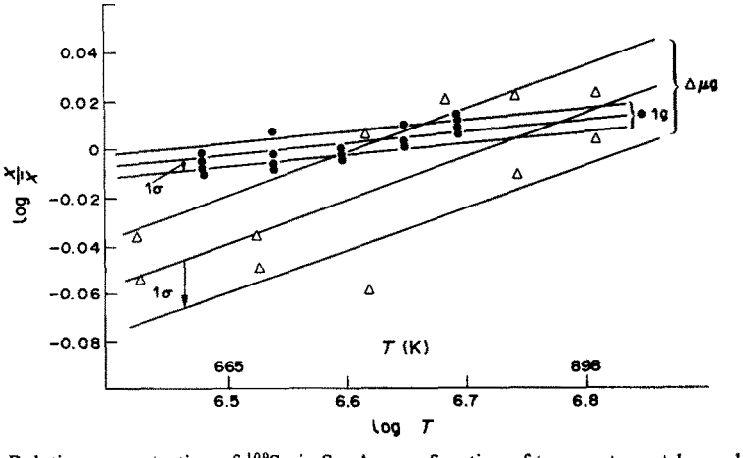

FIG. 10. Relative concentration of ^{109}Sn in Sn–Ag as a function of temperature at 1 g and in μg.

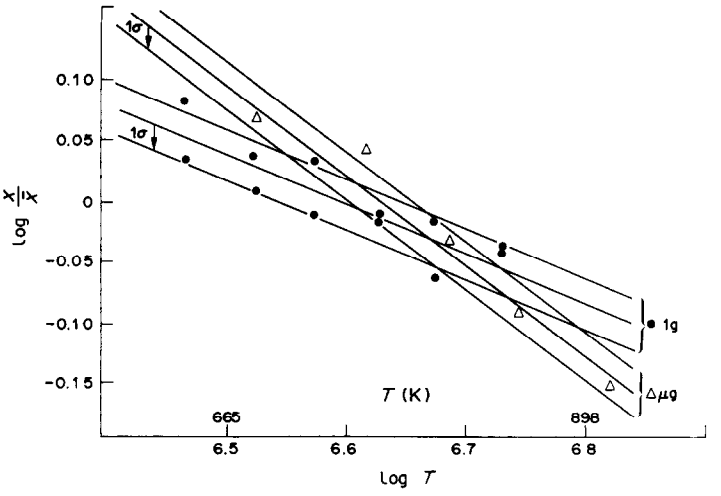

FIG. 11. Relative concentration of Bi in Sn–Bi as a function of temperature at 1 g and in μg.

that

$$(Gr_T)_{lim} = 0.4.$$

Thermal convection. The Grashof number is defined by

$$(Gr)_T = \frac{\gamma \alpha_T (2R_s)^4}{\nu^2} \frac{\partial T}{\partial z} = 9\gamma.$$

Solutal convection. The Grashof number is defined by

$$(Gr)_S = \frac{\gamma \beta_v (2R_s)^4}{\nu^2} \frac{\partial X}{\partial z} \quad \text{with} \quad \frac{\partial X}{\partial z} = \frac{r\bar{X}}{\bar{T}} \frac{\partial T}{\partial z}.$$

Thus

$$\frac{(Gr)_S}{(Gr)_T} = \frac{\beta_v r \bar{X}}{\alpha_T \bar{T}}.$$

This ratio is found to vary from 3×10^{-4} (Sn–Ag system) to 0.2 (Sn–Bi) in these experiments. In all cases, therefore, $(Gr)_S \ll (Gr)_T$.

It then suffices to calculate $(Gr)_T$. Now, γ is of the order of $10^{-6}\, g$ [31].

Thus

$$(Gr)_T = 9\gamma = 10^{-2}$$

and this value is less than $(Gr_T)_{lim} = 0.4$ calculated above.

This analysis shows that $V_c \ll V_d$ or, in other words, the results obtained in microgravity were not significantly disturbed by residual convection.

6.3.2. *Analysis on the basis of three-dimensional numerical calculations by Henry* [16]. Appendix B gives details of the application of these calculations to these experiments. They are summarized in Table 3.

These results are obtained in the most adverse case: residual acceleration perpendicular to the sample axis.

With the continuous component of γ being of the order of $10^{-6}\, g$, the separation efficiency is equal to 1, thus confirming the results obtained by the simplified analysis described in the above section.

7. COMPARISON OF GROUND AND MICROGRAVITY RESULTS

The results clearly indicate that, for all the systems studied, the relative variation in concentration as a function of temperature is greater in μg than at 1 g.

The position of representative points of ground experiments on the diagram (Grashof, solutal Rayleigh number) is shown on Fig. 4(a).

As $r_{\mu g}$ is known, the solutal Rayleigh number corresponding to the ground experiments can be calculated (see Table 4).

For Au in Sn–Au, as no microgravity measurement results are available, the r value obtained for Sn +6%

Table 3. Separation efficiency as a function of residual acceleration γ

Residual acceleration, γ (g = 981 cm s^{-2})	$\ll 10^{-4}\, g$	$10^{-3}\, g$	$10^{-2}\, g$
Separation efficiency: $\left(\frac{\text{measured separation}}{\text{separation without convection}}\right)$	1	0.95	0.20

Table 4. Measurement of the thermal factor $r = (\mathrm{d}\log(X/\bar{X}))/(\mathrm{d}\log T)$ on the ground and in microgravity. Calculation of the associated solutal Rayleigh number

System	Measurement at 1 g or μg	Thermal factor		Ra_S solutal Rayleigh number at 1 g			
		$10^3\, r_{1g}$ measured at 1 g	$10^3\, r_{\mu g}$ measured in μg	Solutal coefficient $\beta_v = (\rho - \rho_{Sn})/\rho_{Sn}$	Mean concentration $\bar{X}$ of experiments at 1 g	$Ra_S = 29\times10^4\beta_v\bar{X}r_{\mu g}$(Co) $Ra_S = 5.4\times10^4\beta_v\bar{X}r_{\mu g}$ (other systems)	$r_{1g}/r_{\mu g}$
^{59}Co in Sn–Co	μg FSLP	0±20	1860±40	0.29	4×10^{-4}	62	0
^{112}Sn in Sn–Co	μg FSLP	0±10	74±9	−0.06	10^{-2}		
^{112}Sn in pure Sn	μg D1	2±12	77±8	−0.06	10^{-2}		
^{112}Sn in Sn–Ag	μg D1	17±10	95±15	−0.06	10^{-2}		
^{112}Sn in Sn–Au	μg D1	56±21		−0.06	10^{-2}		
^{109}Ag in Sn–Ag	μg D1	47±10	175±40	0.33	4×10^{-4}	1	0.26
^{110}Ag in Sn–Ag	1 g	70±7 (ref. [2])		0.33	6×10^{-4}		
^{197}Au in Sn–Au	1 g	−182±36	Not available	1.48	6×10^{-4}	−27	0.31†
	1 g	−574±50			6×10^{-2}	−2700	1.00†
^{209}Bi in Sn–Bi	μg D1	−405±10	−758±40	0.44	4×10^{-2}	−718	0.53

†For calculation of these values, see Section 7.

Au can be taken. All the representative points of these experiments (except Sn +6% Au of course) are located in the domain on the (Ra_T, Ra_S) diagram of Fig. 4(a) where convection contributes to the transport process. Table 4 shows that the ratio $r_{1g}/r_{\mu g}$, reflecting the separation efficiency on the ground, increases with $|Ra_S|$.

By plotting the $r_{1g}/r_{\mu g}$ values obtained for $Gr = 0.12$, Fig. 4(b) is obtained, giving the separation efficiency as a function of Ra_S:

$r_{1g}/r_{\mu g} = 0$ for $Ra_S > 10^2$ (convective regime)

$0 < r_{1g}/r_{\mu g} < 1$ for $-10^3 < Ra_S < 10^2$ (convecto-diffusive regime)

$r_{1g}/r_{\mu g} = 1$ for $Ra_S < -10^3$ (diffusive regime).

In all cases, the isotopic separation of Sn itself has a stabilizing effect that is difficult to quantify, and to which are added the other effects, stabilizing or otherwise.

8. COMPARISON OF EXPERIMENTAL RESULTS WITH THE THEORIES OF TRANSPORT BY THERMOTRANSPORT

8.1. *Summary of general principles* [3]

The theories interpret thermotransport either by phenomenological models (analogy with evaporation–condensation processes), or by kinetic models. Of the latter, the model proposed by Bhat and Swalin [25] expresses the heat of transport

$$Q = \frac{\mathrm{d}\log(X/\bar{X})}{\mathrm{d}\left(\frac{1}{RT}\right)} = -RrT \tag{4}$$

in the form

$$Q = Q_m + Q_e = AT + BT^2 \tag{18}$$

where $Q_m = AT$ is the intrinsic contribution resulting from collisions between ions and $Q_e = BT^2$ the electron contribution resulting from interactions between conduction electrons and alloying elements.

Let $\alpha = -A/R$ and $\beta = -B/R$, then

$$r = \frac{\mathrm{d}\log(X/\bar{X})}{\mathrm{d}(\log T)} = \alpha + \beta T \tag{19}$$

and by integrating equation (19) we have

$$\log(X/\bar{X}) = \alpha\log T + \beta T + C. \tag{20}$$

The coefficient α expresses the mass effect and is calculated from Chapman and Cowling's formula [32]

$$\alpha = -C\left[\frac{m_1 - m_2}{m_1 + m_2} + 0.2x_1\left(\frac{s_1^2}{s_{12}^2} - 1\right) - 0.2x_2\left(\frac{s_2^2}{s_{12}^2} - 1\right)\right] \tag{21}$$

where m_1, m_2 are the atomic weights of solute and solvent, x_1, x_2 the atomic fractions of solute and solvent, s_1, s_2 the equivalent ion diameters, and $s_{12} = (s_1+s_2)/2$ the rigid spheres model. The value of C depends on interactions between atoms and, as a first approximation can be considered to be independent of atomic weight and valency [25]. The coefficient β expresses the electron effect.

For a low concentration (<1%) of solute (1) in solvent (2), ref. [2] gives

$$\beta = -\frac{Z}{R}\frac{\pi^2 k^2 T^2}{3E_F}\left|\frac{\rho_2\varepsilon_2 - \rho_1\varepsilon_1}{\rho_2}\right| \qquad (22)$$

where Z is the mean number of conduction electrons per alloy atom, R the gas constant, k Boltzmann's constant (per atom), E_F the Fermi energy, ρ_1, ρ_2 the electrical resistivities, and $\varepsilon_i = -|(\delta \log \rho_i)/(\delta \log E)|_{E_F}$.

Note on the solutal stability of binary systems. In general, the electron effect is weak compared to the mass effect and r has the same sign as (m_2-m_1) (see equation (21)). In addition $\beta = (\rho_1-\rho_2)/\rho_2$ and the solutal Rayleigh number is the sign of βr (cf. Section 4.1.1).

Most of the systems have physical properties such that (m_1-m_2) and $(\rho_1-\rho_2)$ have the same sign (and thus $Ra_S < 0$), or in other words, solutal stabilizing. Sn–Co or Sn–Ag systems are exceptions to the rule in this respect.

8.2. *Comparison of measurements with the formulation in Section* 8.1

8.2.1. *Measurements concerning* ^{112}Sn. Measurements of ^{112}Sn in pure Sn, in Sn–Ag and in Sn–Co are consistent (see Table 4). These measurements are particularly interesting for the modelling procedure described in Section 8.1 as the electron effect is zero for isotopes and the intrinsic effect (cf. equation (21)) reduces to

$$r = \alpha = -C\frac{m_1-m_2}{m_1+m_2}. \qquad (21')$$

The C value corresponding to the measured r value $(77\pm8)\times10^{-3}$ is

$$C = 2.66\pm0.26.$$

The C value can be used to calculate the values of α for other elements by means of equation (21'). This value of $C = 2.66$ should be compared to:

$C = 5.4$ proposed by Rabinovitch [21] for different isotope mixtures and used by Balourdet [2],

$C = 2.2$ proposed by Bhat and Swalin [25].

The latter value is the average of five close values calculated from experimental results of alloy isotope separation as detailed in Table 5.

It should be noted that refs. [19, 20] indicate that the experiments were performed in 0.6 mm diameter quartz tubes, i.e. under the best possible conditions for minimizing radial temperature gradients (cf. Section 4.3.1).

8.2.2. *Measurements concerning the other systems.* The experimental results were processed by linear regression between $\log(X/\bar{X})$ and $\log T$, with the assumption that the electron effect is negligible compared to the intrinsic contribution for these systems (equation (19)), at least in the temperature range considered.

Table 6 shows that, for ^{109}Ag, ^{197}Au and ^{209}Bi, there is good agreement between the r values cal-

Table 5. C values deduced from measurements on various isotope mixtures

Metal	Atom weight (g)	Sample diameter (mm)	C	References
Li (6–7)	7	2.0	2.03	[18]
K (39–41)	39	0.6	1.93	[19]
Rb (85–87)	85.5	0.6	2.54	[19]
Ga (69–71)	69.7	0.6	2.38	[19]
In (113–115)	114.8	0.6	2.11	[20]

Table 6. Comparison of r values measured under convection-free conditions and values calculated with $C = 2.66$

Solute	Calculated value of $r = \alpha$ equation (21) with $C = 2.66$	Measured value of $r = \mathrm{d}\log(X/\bar{X})/\mathrm{d}(\log T)$	Measurement
^{59}Co	1056×10^{-3}	$(1860\pm40)\times10^{-3}$	μg
^{109}Ag	196×10^{-3}	$(175\pm45)\times10^{-3}$	μg
^{197}Au	-574×10^{-3}	$(574\pm50)\times10^{-3}$	$1g$
^{209}Bi	-768×10^{-3}	$(758\pm66)\times10^{-3}$	μg

culated in this way and the measured r values and therefore gives reasonable confirmation, at least for these three systems, to:

- the hypothesis in which the electron contribution is negligible compared to the intrinsic contribution,
- the validity of formula (21), used with the C value deduced from isotope measurements.

8.2.3. *Particular case of the* Sn–Co *system* [7]. For this system, microgravity experimental results were available from six samples. The accuracy on relative concentration is of the order of 1%, while temperature measurements are accurate to within $\pm 10°C$. A slight curvature can be discerned on Fig. 7, probably due to the electron contribution ($\beta > 0$).

However, results over a much wider temperature range would be necessary in order to calculate α and β with reasonable accuracy [30].

Thus, in spite of the accuracy of the results (indeed, to the author's knowledge, the most accurate found in the literature on this system), it is not possible to determine which of the following reasons is valid for explaining the difference between the calculated value and the measured value of r:

- non-negligible electron contribution compared to the mass contribution,
- for a system including a transition element (Co), non-validity of equation (21) with respect to specific structural factors,
- or a combination of both causes.

8.2.4. *Measurements given in the literature.* Appendix C includes a table of measurements of transport heat Q made on 32 systems [8]. These are compared to the mass contribution Q_m calculated according to formula (21).

When atomic weights differ by more than 10%, as is the case for most of the systems quoted, the electron contribution must be negligible compared to Q_m and the measured Q value must be close to Q_m. Now this is the case only for Ag–Au [24], Au–Ag [29] and K–Na [29]. In some cases, even the direction of solute migration (given by the sign of Q) is not the same between experimental findings and calculations.

The measurement can be disturbed by at least three artefacts described hereafter.

(1) The solute, or a compound formed between solute and solvent, may not be completely dissolved and may concentrate, by sedimentation, at the top or bottom of the sample. In some of the preliminary experiments described here, on Sn–Co, the undissolved compounds of CoSn and $CoSn_2$ sedimented in the cold zone, leading to false measurements of Co concentration in this zone. This fact might explain such results as those described in ref. [22].

(2) In most of the experiments listed, samples were not taken in the liquid state and the temperature holding period is terminated by 'quenching'. A solidification-linked segregation profile may then be superimposed on that due to thermotransport. This effect was observed in certain of the present author's experiments, where the shearing system did not work.

(3) Even if all the precautions are taken to avoid the artefacts described above, convection may still disturb the partial or total diffusion, as explained in preceding sections.

Most authors indicate a mean value of Q independent of temperature.

The electron contribution values are generally estimated by determining the difference between the measured Q value (with all the risks of error described above), and the Q_m value calculated according to equation (21) (which is not necessarily satisfied for all systems).

For the Sn–Ag system, Balourdet *et al.* [3] attempted to interpret their results (concerning 21 experiments) according to equation (18). However, their measurements were disturbed by convection, as shown in Section 7.

Regardless of the method used for deducing the electron contribution in experimental results, the value obtained *has a very low reliability level*, at best of the order of magnitude Q_e. Under these conditions, it would therefore seem illusory to use this value as a basis for confirming the theories enabling Q_e to be calculated from the physical properties of the elements (equation (22)).

Moreover, these theories call for complex models [4] and, in the Q_e calculation, require the introduction of parameters that are difficult to measure, such as partial structure factors or pseudopotentials [3].

In order to have any chance of separating the electron effects from the mass effects, reliable measurements will have to be available, undisturbed by convection (and thus possibly obtained in microgravity) and over a wide temperature range.

9. CONCLUSIONS

It has been shown that the experimental conditions to be obtained on the ground to carry out thermotransport measurements without convection disturbance, can be determined by convection analysis of a given metallic system.

If these conditions cannot be satisfied, the only way to obtain correct measurements is in microgravity. The most immediate benefit of these measurements is that they can be taken into account in solidification models. In such a case, it is sufficient to know the heat of transport to within a few percent in the effective temperature range.

From a more fundamental point of view, if these measurements were to be used to confirm a particular theory on transport mechanisms, then it will be necessary to choose systems with well-known physical and thermodynamic parameters and to be able to conduct accurate measurements over an extensive temperature range.

Finally, for a more applied purpose, it would be possible to consider using thermotransport in microgravity in order to separate certain isotopes.

Acknowledgements—The author gratefully acknowledges the assistance of: Mr Malmejac, who initiated thermotransport studies under microgravity conditions and subsequently monitored and encouraged follow-up work; Mr Favier who urged the author to analyse more particularly the effect of convection on atomic transport measurements; the CNES/GERME team which contributed to the preparation of the space experiments; Messrs Lloret and Bolliet (Piles/CENG) who carried out the activation analyses; Mr Henry (University of Lyon 1) as well as Messrs Camel, Favier and Rouzaud (CENG) for their participation in the convection analysis; Messrs Abadie and Borgis, largely responsible for technical implementation of the experiments, and Mr Gilly who contributed to the analysis of experimental results; G. A. Sumner, professional translator, who translated the text into English and was responsible for page make-up and print-out. This work was carried out within the context of the GRAMME agreement concluded between the C.E.A.–I.R.F. and the C.N.E.S.

REFERENCES

1. C. Potard, Contribution à la diffusion dans les alliages ternaires, Thesis Grenoble (1972).
2. M. Balourdet, Contribution à l'étude des mécanismes de thermodiffusion dans les métaux et alliages liquides, Thesis Grenoble (1976).
3. M. Balourdet, Y. Malmejac and P. Desre, Thermotransport of Ag, In and Sb in liquid Sn, *Phys. Lett.* **56A**(1), 5152 (1976).
4. M. Gerl, Contribution au calcul des forces agissant sur une impureté d'un métal soumis à un gradient de température, *J. Phys. Chem. Solids* **28,** 725–736 (1967).
5. J. P. Praizey et J. Berthier, Problèmes posés par l'intégration d'expériences de science des matériaux dans un véhicule spatial, *Proc. Third European Symp. on Material Sciences in Space*, Grenoble, France, 24–27 April 1979, ESA SP-142, pp. 415–425 (1979).
6. J. P. Praizey, Technical implications of a flight design, *Proc. 4th European Symp. on Material Sciences under Microgravity*, Madrid, 5–8 April 1983 (Edited by T. D. Guyenne and J. Hunt), ESA SP-191, pp. 127–132. ESTEC Reproduction Services, Noordwijk, The Netherlands (1983).
7. Y. Malmejac and J. P. Praizey, Thermomigration of cobalt in liquid tin (1 ES 320), *Proc. 5th European Symp. on Material Sciences under Microgravity*, Schloss Elmau, F.R.G., 5–7 November (Edited by T. D. Guyenne and J. Hunt), ESA Sp-222, pp. 147–152. ESTEC Reproduction Services, Noordwijk, The Netherlands (1984).
8. J. P. Praizey, Thermomigration in liquid metallic alloys, XXVIth COSPAR, Toulouse, France, 30 June–12 July 1986, *Adv. Space Res.* **6**(5), 51–60 (1986).
9. J. P. Praizey, Thermomigration dans les alliages métalliques liquides, *Proc 6th European Symp. on Material Sciences under Microgravity Conditions*, Bordeaux, France, 2 5 December 1986, ESA SP-256, pp. 501–508 (1987).
10. G. Z. Gershuni and E. M. Zhukhovitskii, *Convective Stability of Incompressible Fluids*. Izdatel stvo nauka, Moscow (1972).
11. P. F. Linden, *Convective Transport and Instability Phenomena* (Edited by J. Zierep and H. Oertel), p. 171. Braun, Karlsruhe (1982).
12. J. E. Hart, On sideways diffusive instability, *J. Fluid Mech.* **49**(2), 279–288 (1971).
13. D. Camel and J. J. Favier, Thermal convection and longitudinal macrosegregation in horizontal Bridgman crystal growth, *J. Crystal Growth* **67,** 57–67 (1984).
14. A. Rouzaud, Influence des convections thermique et thermosolutale sur les ségrégations observées lors de la croissance cristalline d'alliages Ge–Si et Ge–Ga, Thesis Grenoble (1984).
15. D. Camel and J. J. Favier, Scaling analysis of convective solute transport and segregation in Bridgman crystal growth from the doped melt, *J. Physique* **47,** 1001–1014 (1986).
16. D. Henry, Simulation 3D des mouvements de convection thermosolutale d'un mélange binaire. Influence sur la séparation par effect Soret, Thesis Lyon (1986).
17. D. Henry and B. Roux, Three-dimensional numerical study of convection in a cylindrical thermal diffusion cell: its influence on the separation on constituents, *Physics Fluids* **29**(11), 3562–3572 (1986).
18. A. Ott and A. Lundeen, Thermal diffusion of isotopes in pure molten Li metal, *Z. Naturf.* **19a,** 822 (1964).
19. A. Lodding and A. Ott, Isotope thermotransport in liquid K, Rb and Ga, *Z. Naturf.* **21a,** 1344 (1966).
20. A. Ott, L. Lowenberg and A. Lodding, Isotope thermotransport in liquid In, *Z. Naturf.* **22a,** 2112 (1967).
21. G. D. Rabinovitch, Approximate evaluation of the thermal diffusion constant in liquid isotopic mixtures, *Inzh.-fiz. Zh.* **15**(6), 1014 (1968).
22. D. K. Belashchenko *et al.*, Diffusion de ^{60}Co and ^{63}Ni dans les bains de fusions métalliques liquids, *Izv. Vuz. Chernaya Metallurgiya* **1,** 5–8 (1968).
23. P. P. Kuz'menko et L. P. Golovinskiy, Thermodiffusion d'impuretés dans le thallium liquide, *Fiz. Metal. Metalloved* **30,** 1304 (1970).
24. B. N. Bhat and R. A. Swalin, Thermotransport of solutes in liquid silver, *Z. Naturf.* **26a,** 45 (1971).
25. B. N. Bhat and R. A. Swalin, Thermotransport of silver in liquid gold, *Acta Met.* **20,** 1387 (1972).
26. B. N. Bhat and R. A. Swalin, Thermotransport of cobalt in liquid silver, *Scripta Met.* **6,** 523–528 (1972).
27. P. P. Kuz'menko et L. P. Golovinskiy, Thermodiffusion d'impuretés dans le cadmium liquide, *Fiz. Metal. Metalloved* **21,** 436 (1972).
28. B. N. Bhat, Thermotransport in liquid Al–Cu alloys. NASA Technical Report R-415 (1973).
29. S. P. Murarka, T. Y. Kim, M. Y. Hsieh and R. A. Swalin, Thermotransport studies in liquid alkali metal alloys, *Acta Met.* **22,** 185–189 (1974).
30. L. Gilly et J. P. Praizey, Dépouillement des expériences de thermodiffusion, SEM Internal Report No. 29/87 (1987).
31. H. Hamacher, R. Jilg (DFVLR Cologne, F.R.G.), and U. Merbold (ESA Paris, France), Analysis of microgravity measurements performed during D1.
32. S. Chapman and T. G. Cowling, *The Mathematical Theory of Non-uniform Gases*. Cambridge University Press, London (1952).
33. Y. Malmejac and G. Frohberg, Mass transport by diffusion. In *Fluid Sciences and Materials Science in Space, a European Perspective* (Edited by H. U. Walter (ESA Paris)), Chap. V, pp. 159–190. Springer, Berlin (1987).

APPENDIX A

This appendix examines the application of Henry's convection analysis [16] to the ground experiments performed. Chapter VI of ref. [16] proposes a three-dimensional convection study in relation to the inclination δ of the sample axis with respect to the vertical.

ΔT_R corresponding to δ is given by

$$\Delta T_R = \Delta T_{axial} \frac{R_s}{L} \sin \delta = 0.14\delta \quad (\delta \text{ in deg})$$

where $\underline{S}$ is the separation parameter defined by

$$\underline{S} = \frac{\beta_v}{\alpha_T} \bar{X}(1-\bar{X}) \frac{r}{T}.$$

From this expression, a separation efficiency better than 99% is obtained for $\delta < 10\underline{S}$ (δ in deg) or $\Delta T_R(\mathrm{K}) < 1.45\underline{S}$.

APPENDIX B

This appendix examines the application of Henry's convection analysis [16] to the microgravity experiments performed. Reference [17] will need to be consulted in order to gain a proper understanding to this appendix, the notations used from this reference being underlined when they do not have the same meaning as in the present text.

The following definitions are thus made:

$$X_{bot} = \text{separation efficiency} = \frac{\text{measured separation}}{\text{separation without convection}}$$

$$\underline{Gr} = \frac{\alpha_T R_s^4}{\nu^2} \frac{\partial T}{\partial z} \gamma = 0.55\gamma$$

(characteristic distance is R_s and not $2R_s$ as in Section 6.3.1)

$$\underline{S} = \frac{\beta_v}{\alpha_T} \bar{X}(1-\bar{X}), \quad S = \frac{\beta_v}{\alpha_T} \bar{X}(1-\bar{X}) \frac{r}{T}$$

$$\alpha_T = 0.85 \times 10^{-4}\ \mathrm{K}^{-1}$$

$$\bar{T} = 750\ \mathrm{K}.$$

For $\underline{S}$ values of the order of 10^{-3}–10^{-4}, reference can be made to Figs. 4, 5 and 17 with $\underline{S} = 0$. For Sn–Bi, it is considered that $\underline{S} = 0.2$.

For the $Pr = 0.6$ charts of ref. [17], there is no temperature field deformation. There is even less likelihood of temperature field deformation for the experiments described here ($Pr = 0.01$) and the charts for $Pr = 0.6$ can be validly used.

The charts included in ref. [17] are given for $Sc = 60$. In the experiments treated here, $Sc = 34$. It would therefore be best to refer to a 'transformed' $\underline{Gr}$ value on the charts

$$\underline{Gr}_{tr} = 34/60\underline{Gr}.$$

A value for X_{bot} can be determined for a shape factor $AZ = 6$ on the basis of Fig. 4 or Fig. 5. To calculate X_{bot} for the present experiments ($AZ = 18$), ref. [17] must be used together with formula (9). This leads to Table B2.

Table B1

System	r	β_v	$\bar{X}$	$\underline{S} = -15.7r\beta_v\bar{X}$
Co in Sn–Co	1860×10^{-3}	0.29	4×10^{-4}	-3.38×10^{-3}
^{112}Sn in pure Sn	77×10^{-3}	−0.06	10^{-2}	7.25×10^{-4}
^{109}Ag in Sn–Ag	175×10^{-3}	0.33	4×10^{-4}	-3.62×10^{-4}
^{209}Bi in Sn–Bi	-758×10^{-3}	0.44	4×10^{-2}	2.09×10^{-1}

Table B2. Separation efficiency (X_{bot}) for different systems

			Systems for which $S \sim 0$ (Sn–Co, pure Sn, Sn–Ag)			Sn–Bi system for which $S = 0.2$		
γ	$\underline{Gr}$	$\underline{Gr}_{tr}$	X_{bot} ($AZ = 6$)	X_m [17] ($AZ = 6$)	X_{bot} ($AZ = 18$)	X_{bot} ($AZ = 6$)	X_m [17] ($AZ = 6$)	X_{bot} ($AZ = 18$)
$10^{-4}g$	0.055	0.030	1	1	1	1	1	1
$10^{-3}g$	0.55	0.30	0.97	0.96	0.96	0.95	0.94	0.94
$10^{-2}g$	5.50	3.00	0.33	0.17	0.22	0.32	0.16	0.21

APPENDIX C

Table C1. Bibliographical review of thermotransport measurements

Solvent	Solute	Reference (year)	Sample diameter (mm)	Temperature gradient (K cm^{-1})	Measured temperature range (°C)	Solutal effect†	Calculated heat of transport (mass effect alone)‡ Q_m (cal mol^{-1})	Measured heat of transport§ Q_{exp} (cal mol^{-1})
^{119}Sn	^{60}Co	22 (1968)	1	40	250–410	dest	−1190	1960
	^{63}Ni	22 (1968)	1	45	400–800	dest	−1110	1380
	^{110}Ag	3 (1976)	1.5	100	450	dest	−190	−84
	^{115}In	3 (1976)	1.5	100	450	?	−60	−68
	^{124}Sb	3 (1976)	1.5	100	450	dest	90	−68
^{108}Ag	^{35}S	24 (1970)	0.75	15	1200–1300	st	−3220	−29000
	^{60}Co	26 (1972)	0.75	20	1250–1350	st	−2110	−8400
	^{125}Sb	24 (1970)	0.75	15	1200–1300	dest	720	−6700
	^{195}Au	24 (1970)	0.75	15	1200–1300	st	1930	1690
^{112}Cd	^{60}Co	22 (1968)	1	40	250–450	?	−1220	1230
	^{63}Ni	22 (1968)	1	45	350–800	?	−1130	1390
	^{65}Zn	27 (1972)		100	540	st	−1030	360
	^{110}Ag	27 (1972)		100	450–500	dest	−80	1750
	^{125}Sb	27 (1972)		100	540	dest	260	2760
	^{204}Tl	27 (1972)		90	450–500	st	1080	1000
^{204}Tl	^{60}Co	22 (1968)	1	40	250–410	st	−2150	3100
	^{63}Ni	22 (1968)	1	45	600–800	st	−3080	1150
	^{65}Zn	23 (1970)	0.7	70	550–650	st	−1980	824
	^{117}In	23 (1970)	0.7	60	450–500	st	−980	1090
	^{121}Sn	23 (1970)	0.7	60	450	st	−920	860
	^{209}Bi	23 (1970)	0.7	60	450	st	70	−1500
	^{210}Pb	23 (1970)	0.7	60	350–500	?	70	671
^{209}Bi	^{60}Co	22 (1968)	1	40	250–450	st	−1930	1560
	^{63}Ni	22 (1968)	1	45	250–800	st	−1860	1800
^{207}Pb	^{60}Co	22 (1968)	1	40	300–450	st	−1900	2580
	^{63}Ni	22 (1968)	1	45	300–800	st	−1840	10250
^{115}In	^{60}Co	22 (1968)	1	40	250–410	dest	−1130	1820
	^{63}Ni	22 (1968)	1	30	700–800	dest	−1517	2320
^{128}Te	^{60}Co	22 (1968)	1	20	380–460	st	−1340	5750
	^{63}Ni	22 (1968)	1	45	400–800	st	−1270	1150
^{27}Al	^{67}Cu	28 (1973)	1.3	50	700–800	st	1810	4850
^{197}Au	^{110}Ag	25 (1972)	0.75		965–1065	st	−1640	−1230
^{22}Na	^{42}K	29 (1974)	0.5	15	150–250	dest	1056	<0
	^{86}Rb	29 (1974)	0.5	15	150–250	st	1452	1070
^{42}K	^{22}Na	29 (1974)	0.5	15	150–250	st	−1044	−1080
^{66}Rb	^{22}Na	29 (1974)	0.5	15	150–250	st	−1512	−4570

†Solutal effect: st, stabilizing, $\beta r < 0$, $Ra_S < 0$; dest, destabilizing, $\beta r > 0$, $Ra_S > 0$.
‡Q_m is calculated according to equation (18).
§Q_{exp} is given in the corresponding bibliographical reference.
Note: for $Q > 0$ (corresponding to $r < 0$, see Section 1), the solute moves towards the cold zone, i.e. towards the bottom in the thermally-stabilizing vertical configuration.

INTERET DE LA MICROGRAVITE POUR LA MESURE DES COEFFICIENTS DE THERMODIFFUSION DANS LES ALLIAGES METALLIQUES LIQUIDES

Résumé—Après un rappel sur la thermodiffusion, on décrit la technique expérimentale utilisée et on présente les résultats obtenus au sol. On détermine les conditions de stabilité solutale auxquelles un alliage métallique doit satisfaire pour que les mesures de thermodiffusion au sol ne soient pas perturbées par la convection. On montre l'intérêt de la microgravité lorsque ces conditions ne peuvent être remplies et on présente les résultats obtenus lors des missions Spacelab de 1983 et 1985 pour Sn pur (séparation isotopique), Sn–Co, Sn–Ag et Sn–Bi. Les résultats des expériences non perturbées par la convection sont comparés à ceux de la littérature (expériences ou calculs effectués à partir de modèles sur la structure des liquides).

DER NUTZEN DER MIKROGRAVITATION BEI DER MESSUNG DES THERMODIFFUSIONS-KOEFFIZIENTEN IN FLÜSSIGEN METALLISCHEN LEGIERUNGEN

Zusammenfassung—Nach einem kurzen Überblick über die Grundlagen der Thermodiffusion werden die Versuchstechnik und die Ergebnisse von terrestrisch ausgeführten Experimenten beschrieben. Es werden Stabilitätsbedingungen angegeben, die erfüllt werden müssen, wenn terrestrisch ausgeführte Messungen der Thermodiffusion nicht durch Konvektionseffekte gestört werden sollen. Der Nutzen der Mikrogravitation wird für Fälle demonstriert, in denen diese Bedingungen nicht erfüllt werden können. Es werden die während der SPACELAB-Missionen 1983 und 1985 erhaltenen Ergebnisse für reines Sn (Isotropentrennung), Sn–Co, Sn–Ag and Sn–Bi präsentiert. Die Ergebnisse der Experimente, die ohne den störenden Einfluß der Konvektion ausgeführt wurden, werden mit in der Literatur gefundenen Werten verglichen (aus Experimenten oder Berechnungen für Flüssigkeits-Struktur-Modelle).

ПРЕИМУЩЕСТВА МИКРОГРАВИТАЦИИ ПРИ ИЗМЕРЕНИИ КОЭФФИЦИЕНТОВ ТЕПЛОПЕРЕНОСА В ЖИДКИХ МЕТАЛЛИЧЕСКИХ СПЛАВАХ

Аннотация—После краткого обзора законов теплопереноса описан используемый экспериментальный метод и представлены результаты, полученные в земных условиях. Предполагается, что металлический сплав удовлетворяет условиям растворимости, и поэтому измерения теплопереноса в земных условиях не нарушаются из-за конвекции. Показаны преимущества микрогравитации в случаях, когда данные условия недостижимы, и представлены результаты, полченные на чистых Sn (разделение изотопов), Sn–Co, Sn–Ag и Sn–Bi при исследованиях в космосе в 1983 и 1985 гг. Результаты экспериментов, проведенных при отсутствии возмущающего эффекта конвекции, сравниваются с имеющимися в литературе данными (экспериментов или расчетов, выполненных по моделям жидких структур).